arXiv:1601.07135v1 [cond-mat.mes-hall] 26 Jan 2016

Observation of an Anisotropic Wigner Crystal

Yang Liu, S. Hasdemir, L.N. Pfeiffer, K.W. West, K.W. Baldwin, and M. Shayegan
Department of Electrical Engineering, Princeton University, Princeton, New Jersey 08544
(Dated: October 2, 2018)

We report a new correlated phase of two-dimensional charged carriers in high magnetic fields, manifested by an anisotropic insulating behavior at low temperatures. It appears near Landau level filling factor $\nu = 1/2$ in hole systems confined to wide GaAs quantum wells when the sample is tilted in magnetic field to an intermediate angle. The parallel field component ($B_{||}$) leads to a crossing of the lowest two Landau levels, and an elongated hole wavefunction in the direction of $B_{||}$. Under these conditions, the in-plane resistance exhibits an insulating behavior, with the resistance along $B_{||}$ more than 10 times smaller than the resistance perpendicular to $B_{||}$. We interpret this anisotropic insulating phase as a two-component, striped Wigner crystal.

Low-disorder, two-dimensional (2D) systems of charged carriers, cooled to low temperatures and subjected to a strong perpendicular magnetic field ($B_\perp$) are host to a plethora of exotic, quantum many-body states [1–3]. At odd-denominator fractional fillings of the lowest Landau level (LL), they exhibit fractional quantum Hall states (FQHSs), uniform-density, incompressible liquid phases for which the resistance vanishes as temperature T approaches absolute zero [1–3]. On the other hand, when the filling factor becomes very small ($\nu \lesssim 1/5$), the system condenses into an ordered array of electrons, the so-called Wigner crystal, which is insulating because it is pinned by the ubiquitous disorder potential [2–8]. Yet another set of states are the anisotropic phases observed at large even-denominator fillings (e.g., $\nu = 9/2$) which are believed to be nematic liquid states [9–12]. The new correlated phase we report here is distinct from these states as it shows an *anisotropic insulating* behavior. It is manifest at low fillings (near $\nu = 1/2$) in 2D hole systems (2DHSs) with a bilayer charge distribution and tilted in magnetic field to introduce a field component ($B_{||}$) parallel to the 2D plane. Curiously, the anisotropic phase forms in a relatively narrow range of tilt angles near $\theta \simeq 35^\circ$ when the two lowest energy LLs are very close in energy. Outside this range, the 2DHS is not insulating and exhibits FQHSs at numerous fillings. The conditions under which the new insulating phase appears suggest that it is an anisotropic (striped), two-component, pinned Wigner crystal (Fig. 1(a)).

Our 2DHSs are confined to 40- and 50-nm-wide GaAs quantum wells (QWs) flanked by undoped $Al_{0.3}Ga_{0.7}As$ spacer and C δ-doped layers, and have as grown densities $\simeq 1.2 \times 10^{11}$ cm^{-2}. The structures were grown by molecular beam epitaxy on GaAs (001) wafers and have very high low-temperature mobilities, $\mu \gtrsim 100$ m^2/Vs. Each sample has a 4×4 mm^2 van der Pauw geometry with alloyed In:Zn contacts at its four corners. We then fit it with an evaporated Ti/Au front-gate and an In back-gate to control the 2DHS density (p) and keep the QW symmetric. The holes in the QW have a bilayer-like charge distribution (Fig. 1(b)). The transport measurements were carried out in a dilution refrigerator with a base temperature of $T \simeq 30$ mK, and an *in-situ* rotatable sample platform to induce $B_{||}$. As illustrated in Fig. 1(c), we use θ to express the angle between the field and the sample plane normal, and denote the longitudinal resistances measured along and perpendicular to the direction of $B_{||}$ by R_{xx} and R_{yy}, respectively. We used low-frequency (~ 30 Hz) lock-in technique to measure the transport coefficients.

Figure 1 (e) highlights our main finding. It shows the longitudinal (R_{xx} and R_{yy}) and Hall (R_{xy}) magnetoresistance traces, measured for a 2DHS confined to a 40-nm-wide GaAs QW at $p = 1.28 \times 10^{11}$ cm^{-2} and $\theta \simeq 35^\circ$. Starting at $B \simeq 8$ T, both R_{xx} and R_{yy} rapidly increase; note the 50 times change of scale for R_{xx} and R_{yy} above 8 T [13–15]. Most remarkably, near $\nu = 1/2$, R_{xx} is ~ 25 kΩ while $R_{yy} \simeq 10 R_{xx}$ and, as we will show shortly, both R_{xx} and R_{yy} exhibit an insulating behavior. To probe the origin of this anisotropic insulating phase (IP), we present several experimental observations.

Data of Fig. 2, which were taken at $\theta = 0$ and 50°, demonstrate that the anisotropic IP seen in Fig. 1(e) occurs near a crossing of the lowest two LLs (Fig. 1(d)). The crossing is signaled by a profound weakening of the $\nu = 1$ integer QHS at intermediate θ [16, 17]. As is evident in Fig. 2, traces taken at both $\theta = 0$ and 50° show a strong integer QHS at $\nu = 1$, with a very wide resistance plateau and large excitation gap $\Delta \gtrsim 10$ K. In contrast, at intermediate angle $\theta \simeq 35^\circ$ (Fig. 1(e)), the $\nu = 1$ QHS becomes much weaker ($\Delta \simeq 0.22$ K) and has a very narrow plateau.

The evolution of the FQHSs in Figs. 1(e) and 2 are also consistent with a LL crossing occurring near $\nu = 1$ when $\theta \simeq 35^\circ$. In Fig. 2 traces there are numerous strong FQHSs at the well-known, "standard" $\nu = i/(2i \pm 1)$ fillings ($i > 0$ is an integer) [3]. In Fig. 1(e) data, however, near $\nu = 1$ there are uncharacteristically strong FQHSs at the *even-numerator* fillings $\nu = 4/3$, $6/5$, $6/7$, and $4/5$. This is similar to what is seen in bilayer 2D *electron* systems (2DESs) with extremely small energy separation between the lowest two LLs [18], and implies that these are two-component FQHSs, each component having half of the total filling. In Fig. 1(e) we also observe

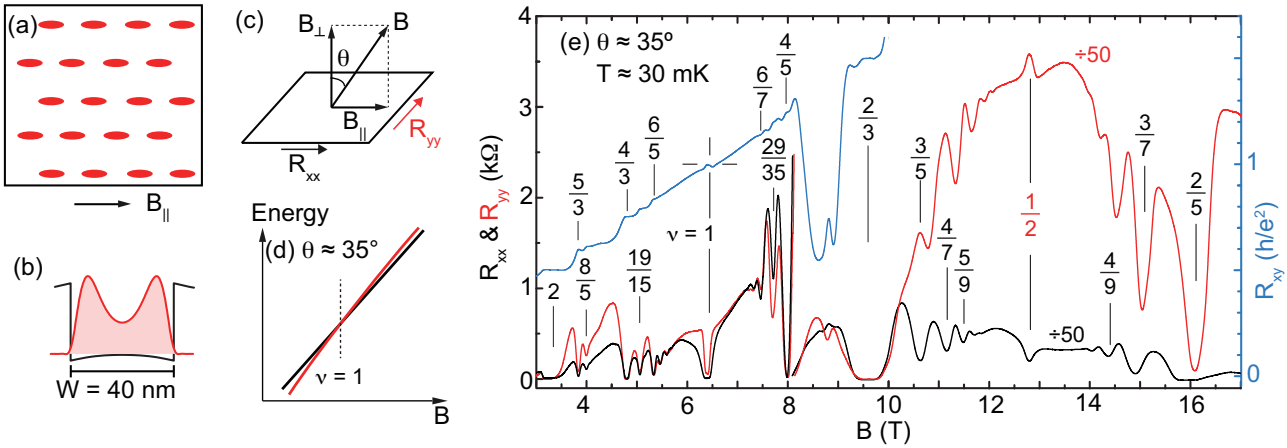

FIG. 1. (color online) (a) Conceptual plot of an anisotropic (striped) Wigner crystal. (b) The charge distribution (red) and potential (black), from calculating the Schroedinger and Poisson's equations self-consistently at $B = 0$. (c) Experimental geometry: R_{xx} and R_{yy} denote the longitudinal magneto-resistance measured along and perpendicular to the parallel magnetic field ($B_{||}$), respectively. (d) Schematic diagram, showing the crossing of the lowest two Landau levels at $\theta \simeq 35^\circ$ near $\nu = 1$. (e) Magneto-resistance traces measured at tilt angle $\theta \simeq 35^\circ$ for a 2DHS with density $p = 1.28 \times 10^{11}$ cm^{-2} and confined to a 40-nm-wide GaAs QW. Note the factor of 50 change in the scale for R_{xx} and R_{yy} for $B > 8$ T.

FQHSs at very unusual fillings such as $\nu = 19/15$ and $29/35$. Such states were seen in Ref. [18] when the lowest two LLs are nearly degenerate, and were interpreted as "imbalanced" two-component FQHSs: for example, the $\nu = 19/15$ FQHS has fillings $2/3$ and $3/5$ for its two components. In Fig. 2, we also observe strong FQHSs at the even-denominator filling $\nu = 1/2$. This FQHS is seen in 2DESs and 2DHSs confined to wide GaAs QWs [19–22]. It is likely the Ψ_{331} state, a two-component FQHS stabilized by strong and comparable interlayer and intralayer interactions which are prevalent at $\nu = 1/2$ [23].

Next we focus on the anisotropic IP seen at $\theta \simeq 35^\circ$. Figure 3 captures the insulating behavior of this phase near $\nu = 1/2$. Both R_{xx} and R_{yy} increase as temperature is decreased but, as can be best seen in Fig. 3(b), R_{yy} is about 10 times larger than R_{xx}. Before discussing this anisotropic behavior, it is instructive to first briefly review the IPs seen in 2D systems at low fillings.

It is well established that in very clean 2D systems of charged carriers, at very small ν ($\nu \lesssim 1/5$ for electrons and $\nu \lesssim 1/3$ for holes) the FQHSs give way to IPs which are believed to be Wigner crystal (WC) phases that are pinned by the small but ubiquitous disorder [4–7, 24–27]. For both 2D electron and hole systems in wide, symmetric GaAs QWs, the charge distribution becomes more bilayer-like with increasing density and the IP sets in at progressively larger ν [22, 28, 29]. These IPs are believed to be *bilayer* WC states which, thanks to the additional layer/subband degree of freedom, are stabilized at relatively large ν compared to the single-layer systems. For example, in 2DHSs confined to a 40-nm-wide QW with $p \gtrsim 1.7 \times 10^{11}$ cm^{-2} [22], an IP is observed near $\nu = 1/2$. All the IPs described above are *isotropic*, and were observed in the absence of $B_{||}$ [30, 31].

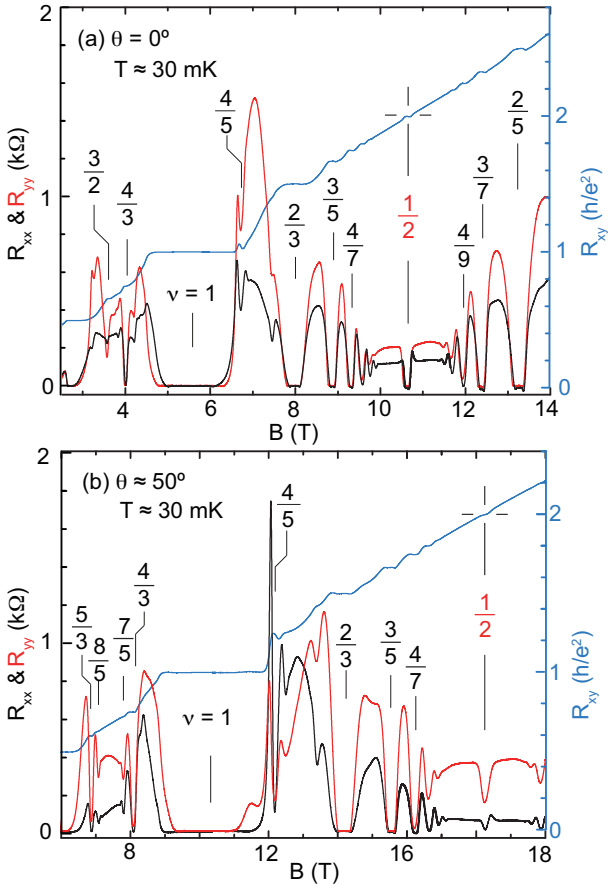

FIG. 2. (color online) Magneto-resistance traces for the sample of Fig. 1, measured at $\theta = 0^\circ$ and 50°. Both R_{xx} and R_{yy} are much smaller near $\nu = 1/2$ than in Fig. 1(e) data.

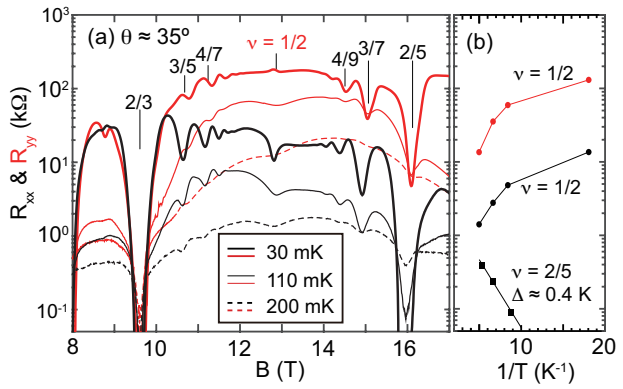

FIG. 3. (color online) (a) R_{xx} and R_{yy} measured at three temperatures in the 40-nm-wide QW near $\nu = 1/2$ at $\theta \simeq 35°$. (b) T-dependence of R_{xx} and R_{yy} at $\nu = 1/2$. To avoid the influence of the relatively sharp $\nu = 1/2$ resistance minima seen in some of the traces, here we are plotting the background resistances by interpolating between the shoulders flanking the $\nu = 1/2$ minima. Also plotted is the T-dependence of the R_{xx} minimum for the $\nu = 2/5$ FQHS.

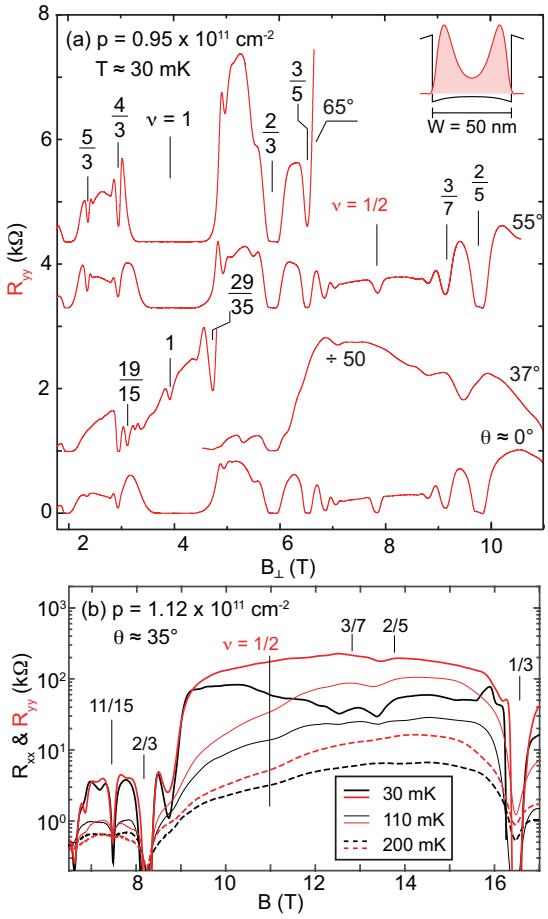

FIG. 4. (color online) (a) R_{yy} vs $B_\perp$ traces measured for a 2DHS confined to a 50-nm-wide GaAs QW at density $p = 0.95 \times 10^{11}$ cm^{-2} and at different θ. The 2DHS exhibits an insulating behavior near $\nu = 1/2$ at $\theta \simeq 37°$ and at $\theta = 65°$, but not at $\theta = 25°$ or $\theta = 55°$. The inset shows the calculated charge distribution and potential at $B = 0$. (b) R_{xx} and R_{yy} traces are shown at $\theta \simeq 35°$ and at a slighlty larger density ($p = 1.12 \times 10^{11}$ cm^{-2}) for different temperatures. Similar to the data of Fig. 3, both R_{xx} R_{yy} exhibit insulating behavior and the system is anisotropic near $\nu = 1/2$.

To discuss the likely origin of the anisotropic IP we observe near $\nu = 1/2$, we focus on its key attributes:

(i) It is a collective state. There are numerous FQHSs near $\nu = 1/2$ in Fig. 1(e), e.g., at $\nu = 2/5$, 3/7, 4/9, 3/5, 4/7, 5/9. These correlated states are much weaker than the FQHSs seen at the same fillings in Fig. 2 traces, but their mere presence in Fig. 1(e) strongly suggests that correlations are prevalent near $\nu = 1/2$ where the IP reigns. Also worth emphasizing is that in Fig. 2 traces there are very strong FQHSs near and even *at* $\nu = 1/2$. It is very unlikely that at the intermediate tilt angle of Fig. 1(e) interactions would disappear and the ground state become of single-particle origin.

(ii) It is a two-component state. It is clear that the anisotropic IP is observed near a LL crossing, and Fig. 2 traces, which were taken far from the LL crossing, do not show insulating behavior near $\nu = 1/2$. This implies that the presence of two nearly degenerate LLs plays a crucial role for its stability. Also, theoretical calculations rule out any single-component WC near $\nu = 1/2$ [32]. The anisotropic IP we observe at $\theta \simeq 35°$ is thus likely to have a two-component origin. In Fig. 3(a), the existence of minima at $\nu = 2/5$, 3/7, 3/5, and their deepening (relative to the insulating background resistance) at lower temperatures, signal a close competition between a reentrant two-component WC phase and the FQHSs. We add that, whether isotropic or anisotropic, one-component or two-component, the observation of an IP near the crossing of two LLs is by itself unprecedented.

(iii) It is not a nematic liquid state. One might naively conclude that the anisotropy we report resembles the one observed at higher half-filled LLs, and believed to signal nematic electron phases [9–12, 33]. But this is incorrect, as there are two major, qualitative differences. First, nematic phases are *liquid* states: while in-plane transport becomes anisotropic, R_{xx} and R_{yy} do not diverge at low temperatures; instead they remain finite and in fact the resistance along the "easy axis" direction decreases as temperature is lowered and attains extremely small values [9, 10]. This is very different from the *insulating* behavior and the large values we measure for both R_{xx} and R_{yy}. Second, in the case of $B_{||}$-induced nematic phases, the "hard axis" is typically along $B_{||}$ [34, 35]. We observe the opposite behavior: the resistance along $B_{||}$ (R_{xx}) is *smaller* than in the perpendicular direction [36].

Based on the above observations, we associate the IP observed in Fig. 1(e) with a pinned, anisotropic WC. We suggest that the anisotropy originates from the strongly distorted shape of the hole charge distribution induced

by $B_{||}$, as schematically depicted in Fig. 1(a). Because of the finite thickness of the hole layer in our sample, $B_{||}$ couples to the out-of-plane (orbital) motion of the carriers, and squeezes the charge distribution in the direction perpendicular to $B_{||}$ (see Fig. 1(a)). Such distortions have been recently documented for carriers near $B_\perp = 0$, and also for composite fermions at high $B_\perp$ [37–39]. An elongated charge distribution can lead to anisotropic interaction, and provides a natural explanation for the anisotropic IP we observe in terms of a pinned, striped WC as shown in Fig. 1(a) [40–42]. Moreover, it is consistent with the experimental observation that the transport "easy axis" is along $B_{||}$ (i.e., $R_{xx} < R_{yy}$), as intuitively the excited quasi-particles (at finite temperatures) should have a higher hopping rate in the direction of charge distribution elongation.

Data taken on the 50-nm-wide QW (Fig. 4) corroborate Figs. 1-3 data and our above conclusions, and reveal new information. In Fig. 4(a) we show R_{yy} traces at density $p = 0.95 \times 10^{11}$ cm^{-2} at different angles. Qualitatively similar to the data of Figs. 1 and 2, the traces at $\theta = 0^\circ$ and 55° appear normal and exhibit a very strong $\nu = 1$ integer QHS and numerous FQHSs at standard fillings as well as at $\nu = 1/2$. The $\theta \simeq 37^\circ$ trace, however, shows an IP near $\nu = 1/2$. The same trace also indicates a weak minimum near $\nu = 1$ and other features, e.g. FQHSs at $\nu = 19/15$ and $29/35$, indicating that the two lowest LLs are near a coincidence. Traces taken at $\theta \simeq 35^\circ$ and slightly higher density, presented in Fig. 4(b), reveal that $R_{yy} >> R_{xx}$ and that both R_{xx} and R_{yy} show insulating behavior near $\nu = 1/2$, similar to the 40-nm-wide QW data of Fig. 3.

The smaller density in the 50-nm QW sample allows us to make measurements at higher tilt angles. As seen in the top trace of Fig. 4(a), taken at $\theta \simeq 65^\circ$, an IP reappears at high $B_\perp$, past $\nu = 3/5$. We believe this IP signals the onset of the 2DHS splitting into a bilayer system, similar to what is seen in 2DESs confined to wide QWs at very large tilt angles [43].

The results we report here attest to the extremely rich physics of 2DHSs confined to wide GaAs QWs. In these systems one can cause a crossing of the lowest two LLs by either changing the density [44] or titling the sample in magnetic field [16, 17, 44]. Depending on the sample parameters, the crossing can destroy the ordinary QHSs, both at integer and fractional fillings, and bring to life unusual phases such as a FQHS at $\nu = 1/2$ [44] or, as we have shown here, an anisotropic IP signaling a two-component, striped Wigner crystal.

We acknowledge support by the DOE BES (DE-FG02-00-ER45841) grant for measurements, and the NSF (Grants DMR-1305691 and MRSEC DMR-1420541), the Gordon and Betty Moore Foundation (Grant GBMF4420), and Keck Foundation for sample fabrication and characterization. We thank R.N. Bhatt, E. Fradkin, J.K. Jain, and S.A. Kivelson for illuminating discussions, and R. Winkler for providing the charge distribution and potential calculations shown in Figs. 1(b) and 4(a). A portion of this work was performed at the NHMFL, which is supported by the NSF Cooperative Agreement No. DMR-1157490, the State of Florida, and the DOE. We thank S. Hannahs, G. E. Jones, T. P. Murphy, E. Palm, A. Suslov, and J. H. Park for technical assistance.

[1] D. C. Tsui, H. L. Stormer, and A. C. Gossard, Phys. Rev. Lett. **48**, 1559 (1982).
[2] M. Shayegan, in *High Magnetic Fields: Science and Technology*, Vol. 3, edited by F. Herlach and N. Miura (World Scientific, Singapore, 2006) pp. 31–60.
[3] J. K. Jain, *Composite Fermions* (Cambridge University Press, Cambridge, UK, 2007).
[4] E. Y. Andrei, G. Deville, D. C. Glattli, F. I. B. Williams, E. Paris, and B. Etienne, Phys. Rev. Lett. **60**, 2765 (1988).
[5] H. W. Jiang, R. L. Willett, H. L. Stormer, D. C. Tsui, L. N. Pfeiffer, and K. W. West, Phys. Rev. Lett. **65**, 633 (1990).
[6] V. J. Goldman, M. Santos, M. Shayegan, and J. E. Cunningham, Phys. Rev. Lett. **65**, 2189 (1990).
[7] M. Shayegan, in *Perspectives in Quantum Hall Effects*, edited by S. D. Sarma and A. Pinczuk (Wiley, New York, 1998) pp. 343–383.
[8] Y. Liu, H. Deng, M. Shayegan, L. N. Pfeiffer, K. W. West, and K. W. Baldwin, arXiv:1410.3435 (2014).
[9] M. P. Lilly, K. B. Cooper, J. P. Eisenstein, L. N. Pfeiffer, and K. W. West, Phys. Rev. Lett. **82**, 394 (1999).
[10] R. R. Du, D. C. Tsui, H. L. Stormer, L. N. Pfeiffer, K. W. Baldwin, and K. W. West, Solid State Communications **109**, 389 (1999).
[11] M. Shayegan, H. C. Manoharan, S. J. Papadakis, and E. P. D. Poortere, Physica E: Low-dimensional Systems and Nanostructures **6**, 40 (2000).
[12] E. Fradkin, S. A. Kivelson, M. J. Lawler, J. P. Eisenstein, and A. P. Mackenzie, Annu. Rev. Condens. Matter Phys. **1**, 153 (2010).
[13] In Fig. 1(e), the anomalous drop in R_{xy} for $8 < B < 9$ T is an artifact due to the mixing of the longitudinal resistances which attain very high values [14, 15].
[14] V. J. Goldman, J. K. Wang, B. Su, and M. Shayegan, Phys. Rev. Lett. **70**, 647 (1993).
[15] T. Sajoto, Y. P. Li, L. W. Engel, D. C. Tsui, and M. Shayegan, Phys. Rev. Lett. **70**, 2321 (1993).
[16] A. L. Graninger, D. Kamburov, M. Shayegan, L. N. Pfeiffer, K. W. West, K. W. Baldwin, and R. Winkler, Phys. Rev. Lett. **107**, 176810 (2011).
[17] Y. Liu, S. Hasdemir, M. Shayegan, L. N. Pfeiffer, K. W. West, and K. W. Baldwin, Phys. Rev. B **92**, 195156 (2015).
[18] H. C. Manoharan, Y. W. Suen, T. S. Lay, M. B. Santos, and M. Shayegan, Phys. Rev. Lett. **79**, 2722 (1997).
[19] Y. W. Suen, L. W. Engel, M. B. Santos, M. Shayegan, and D. C. Tsui, Phys. Rev. Lett. **68**, 1379 (1992).
[20] Y. W. Suen, H. C. Manoharan, X. Ying, M. B. Santos, and M. Shayegan, Phys. Rev. Lett. **72**, 3405 (1994).

[21] J. Shabani, Y. Liu, M. Shayegan, L. N. Pfeiffer, K. W. West, and K. W. Baldwin, Phys. Rev. B **88**, 245413 (2013).

[22] Y. Liu, A. L. Graninger, S. Hasdemir, M. Shayegan, L. N. Pfeiffer, K. W. West, K. W. Baldwin, and R. Winkler, Phys. Rev. Lett. **112**, 046804 (2014).

[23] In Fig. 2(a) we also see a developing FQHS at $\nu = 3/2$, which can be interpreted as the particle-hole counterpart of the $\nu = 1/2$ FQHS. Also, the weak QHS at $\nu = 1$ in Fig. 1(e) is likely the two-component Ψ_{111} state [17].

[24] Y. Lozovik and V. Yudson, JETP Lett. **22**, 11 (1975).

[25] M. B. Santos, Y. W. Suen, M. Shayegan, Y. P. Li, L. W. Engel, and D. C. Tsui, Phys. Rev. Lett. **68**, 1188 (1992).

[26] M. B. Santos, J. Jo, Y. W. Suen, L. W. Engel, and M. Shayegan, Phys. Rev. B **46**, 13639 (1992).

[27] C.-C. Li, L. W. Engel, D. Shahar, D. C. Tsui, and M. Shayegan, Phys. Rev. Lett. **79**, 1353 (1997).

[28] H. C. Manoharan, Y. W. Suen, M. B. Santos, and M. Shayegan, Phys. Rev. Lett. **77**, 1813 (1996).

[29] A. T. Hatke, Y. Liu, L. W. Engel, M. Shayegan, L. N. Pfeiffer, K. W. West, and K. W. Baldwin, Nature Communications **6**, 7071 (2015).

[30] Termination of the FQHSs by IPs at low fillings has also been reported in fixed-density 2DESs confined to wide GaAs QWs when a large $B_{||}$ is applied [31]. In this case, $B_{||}$ couples to the orbital (out-of-plane) motion of electrons and renders the system progressively more bilayer-like with increasing $B_{||}$ [31].

[31] S. Hasdemir, Y. Liu, H. Deng, M. Shayegan, L. N. Pfeiffer, K. W. West, K. W. Baldwin, and R. Winkler, Phys. Rev. B **91**, 045113 (2015).

[32] A. C. Archer, K. Park, and J. K. Jain, Phys. Rev. Lett. **111**, 146804 (2013).

[33] E. Fradkin and S. A. Kivelson, Phys. Rev. B **59**, 8065 (1999).

[34] W. Pan, J.-S. Xia, V. Shvarts, D. E. Adams, H. L. Stormer, D. C. Tsui, L. N. Pfeiffer, K. W. Baldwin, and K. W. West, Phys. Rev. Lett. **83**, 3530 (1999).

[35] M. P. Lilly, K. B. Cooper, J. P. Eisenstein, L. N. Pfeiffer, and K. W. West, Phys. Rev. Lett. **83**, 824 (1999).

[36] Some anisotropy is also seen in Fig. 2 traces. The rather small (less than a factor of two) anisotropy observed in Fig. 2(a) ($\theta = 0^\circ$) near $\nu = 1/2$ possibly comes from the sample's van der Pauw geometry and the contacts' misalignment. The anisotropy becomes larger, about a factor of four, in Fig. 2(b) ($\theta = 50^\circ$). The origin of this increased anisotropy is likely the deformation (elongation) of the hole charge distribution along $B_{||}$ (Fig. 1(a)), as we discuss later in the manuscript.

[37] D. Kamburov, M. Shayegan, R. Winkler, L. N. Pfeiffer, K. W. West, and K. W. Baldwin, Phys. Rev. B **86**, 241302 (2012).

[38] D. Kamburov, Y. Liu, M. Shayegan, L. N. Pfeiffer, K. W. West, and K. W. Baldwin, Phys. Rev. Lett. **110**, 206801 (2013).

[39] D. Kamburov, M. A. Mueed, M. Shayegan, L. N. Pfeiffer, K. W. West, K. W. Baldwin, J. J. D. Lee, and R. Winkler, Phys. Rev. B **89**, 085304 (2014).

[40] An "insulating stripe-crystal" phase has indeed been discussed theoretically for an interacting 2D system in the excited ($N = 2$) LL [33].

[41] The role of effective mass anisotropy for 2D WC states has also been discussed in Ref. [42].

[42] X. Wan and R. N. Bhatt, Phys. Rev. B **65**, 233209 (2002).

[43] See, e.g., the $\theta = 40^\circ$ trace in Fig. 1 of Ref. [31].

[44] Y. Liu, S. Hasdemir, D. Kamburov, A. L. Graninger, M. Shayegan, L. N. Pfeiffer, K. W. West, K. W. Baldwin, and R. Winkler, Phys. Rev. B **89**, 165313 (2014).